Journal of Computational Physics **168,** 131–154 (2001)
doi:10.1006/jcph.2000.6684, available online at http://www.idealibrary.com on IDEAL®

Splitting Techniques with Staggered Grids for the Navier–Stokes Equations in the 2D Case

Heike Haschke and Wilhelm Heinrichs

Ingenieurmathematik (FB 10), Universität GH Essen, D-45117 Essen, Germany
E-mail: hhaschke@ing.math.uni-essen.de

Received November 4, 1999; revised November 6, 2000

A pseudo-spectral approximation for the Navier–Stokes equations in the 2D case is presented using a new splitting technique based on the Uzawa algorithm. The system is decoupled into Helmholtz equations for the velocity and an equation with the pseudo-Laplacian for the pressure. Staggered grids with Gauss– and Gauss–Lobatto nodes are employed. Preconditioning with finite differences is considered. By extrapolation, a stable second-order method in time for the velocity and at least a first-order method for the pressure can be achieved.

1. INTRODUCTION

We present a pseudo-spectral approximation for the Navier–Stokes equations. For simplicity, we first consider the unsteady Stokes equation which is discretized by a Chebyshev collocation method. This means that the solution is approximated by global Chebyshev polynomials (see, e.g., Canuto *et al.* [7]).

Our approach to solve the spectral system is to use a global iterative decoupling procedure. This procedure is an extension of the classical Uzawa algorithm (Arrow *et al.* [1]) which was already extensively used in the finite element context (see Bristeau *et al.* [6], Girault and Raviart [10], Brezzi and Fortin [5], Babuška and Suri [2], and Temam [19]). In the context of spectral element methods, this approach was also chosen by Maday *et al.* [15] and Rønquist [18].

Finally, we present a decoupling where we reduce the problem to the solution of a Helmholtz equation and another equation with the pseudo-Laplacian for the pressure. To avoid spurious modes we introduce two grids by taking the Gauss nodes for the pressure and the standard Chebyshev Gauss–Lobatto nodes for the velocity. Thereby the pressure is approximated by polynomials of one degree less than those used for the velocity. A similar idea was proposed by Bernardi and Maday [3] where three grids are used, one for the pressure and two for the velocity, i.e., one for each velocity component. Their technique based on the use of Legendre polynomials, but without any splitting technique. Moreover, no numerical

0021-9991/01 $35.00

results are presented in [3]. Another method without the use of staggered grids is considered by Heinrichs [12], where the pressure is approximated by polynomials of two degree less than for the velocity. We show that our new approach has better preconditioning properties than the method by Heinrichs described above. In [13] another related method is proposed is where both velocity and pressure are approximated by polynomials of order N. However, this leads to four spurious modes. A large number of related methods using staggered grids can be found in the recent literature. The main difference between these methods and our approach presented here is that we combine staggered grids with an appropriate splitting technique. This has obvious advantages for the implementation and computational cost.

We also prove that the eigenvalues of the spectral pseudo–Laplacian are real and negative (except of one eigenvalue which is zero and belongs to the constant mode). This implies that we have no spurious modes. Since the spectral pseudo–Laplacian is very ill-conditioned we present suitable finite difference (FD) preconditioners for an effective iterative solver.

We transfer our splitting for the unsteady Stokes equation to the Navier–Stokes equations where we have a closer look at the convective term. For the time discretization a high-order backward differentiation scheme for the intermediate velocity is combined with a high-order extrapolant for the pressure. It is numerically shown that a stable second-order method in time for the velocity and at least first order for the pressure can be achieved.

2. TIME SPLITTING SCHEME

We consider the unsteady Stokes equations

$$\frac{\partial u}{\partial t} - \nabla^2 u + \nabla p = f \quad \text{in } \Omega = (-1,1)^2, \tag{2.1}$$

$$\nabla \cdot u = 0 \quad \text{in } \Omega, \tag{2.2}$$

$$u = 0 \quad \text{on } \partial\Omega, \tag{2.3}$$

where $u = (u_1, u_2)^t$ denotes the velocity and p the pressure. The function $f : \Omega \to \mathbb{R}^2$ is a given force. We impose the average pressure to be zero; i.e.,

$$\int_\Omega p \, dx = 0,$$

as the pressure is only determined up to a constant.

The BDF (see [8]) time discretization of Eqs. (2.1)–(2.3) leads to the scheme

$$L^n_{t,k} u^{n+1} - \nabla^2 u^{n+1} + \nabla p^{n+1} = f^{n+1} \quad \text{in } \Omega, \tag{2.4}$$

$$\nabla \cdot u^{n+1} = 0 \quad \text{in } \Omega, \tag{2.5}$$

$$u^{n+1} = 0 \quad \text{on } \partial\Omega, \tag{2.6}$$

where $\triangle t$ denotes the step size in t and the index $n+1$ indicates that the functions are evaluated at the time step $t_{n+1} = (n+1) \cdot \triangle t$. $L^n_{t,k}$ represents the backward differentation scheme for the approximation of $\frac{\partial}{\partial t}$ and k is the order of the scheme. $L^n_{t,k}$ can be written as

$$L^n_{t,k} u^{n+1} = \frac{1}{\triangle t} \sum_{m=0}^{k} \beta_m u^{n+1-m}.$$

For $k = 1$ the standard backward Euler scheme is given by $\beta_0 = 1$, $\beta_1 = -1$ and we obtain

$$L^n_{t,1} u^{n+1} = \frac{u^{n+1} - u^n}{\triangle t}.$$

This algorithm is of first order in time.

A second-order scheme can be obtained for $k = 2$ using $\beta_0 = \frac{3}{2}$, $\beta_1 = -2$, $\beta_2 = \frac{1}{2}$:

$$L^n_{t,2} u^{n+1} = \frac{\frac{3}{2}u^{n+1} - 2u^n + \frac{1}{2}u^{n-1}}{\triangle t}.$$

Finally, a method of third order for $k = 3$ is given applying $\beta_0 = \frac{11}{6}$, $\beta_1 = -3$, $\beta_2 = \frac{3}{2}$, and $\beta_3 = -\frac{1}{3}$.

To minimize the computational cost we introduce the following splitting scheme which was proposed by Maday *et al.* [16]. We obtain

$$L^n_{t,k} \tilde{u}^{n+1} - \nabla^2 \tilde{u}^{n+1} + \nabla \overline{p}^{n+1}_l = f^{n+1} \quad \text{in } \Omega, \tag{2.7}$$

$$\tilde{u}^{n+1} = 0 \quad \text{on } \partial\Omega, \tag{2.8}$$

and

$$\beta_0 \frac{u^{n+1} - \tilde{u}^{n+1}}{\triangle t} + \nabla\left(p^{n+1} - \overline{p}^{n+1}_l\right) = 0 \quad \text{in } \Omega, \tag{2.9}$$

$$\nabla \cdot u^{n+1} = 0 \quad \text{in } \Omega, \tag{2.10}$$

$$u^{n+1} \cdot \nu = 0 \quad \text{on } \partial\Omega. \tag{2.11}$$

Here, ν denotes the outer unit normal, $\tilde{u}^{n+1}$ an intermediate velocity, and $\overline{p}^{n+1}_l$ an extrapolant for the pressure obtained from the previous l time steps.

Obviously the order of convergence depends on the order k of the backward differentiation scheme and on the order l of the extrapolation where

$$\overline{p}^{n+1}_l = \sum_{m=0}^{l-1} \gamma_m p^{n-m},$$

the values γ_m, $m = 0, \ldots, l-1$, being suitable coeffcients. For $l = 1$ we use especially $\gamma_0 = 1$; for $l = 2$ we have $\gamma_0 = 2$, $\gamma_1 = -1$.

Let

$$\tilde{f}^{n+1} = f^{n+1} - \frac{1}{\triangle t} \sum_{m=1}^{k} \beta_m u^{n+1-m} - \nabla \overline{p}^{n+1}_l.$$

Equations (2.7) and (2.8) are equivalent to the following Helmholtz problem:

$$\left(-\nabla^2 + \beta_0 \frac{1}{\triangle t} I\right) \tilde{u}^{n+1} = \tilde{f}^{n+1} \quad \text{in } \Omega, \tag{2.12}$$

$$\tilde{u}^{n+1} = 0 \quad \text{on } \partial\Omega. \tag{2.13}$$

The system (2.9)–(2.11) corresponds to

$$\beta_0 \frac{1}{\triangle t} u^{n+1} + \nabla p^{n+1} = g^{n+1} \quad \text{in } \Omega, \tag{2.14}$$

$$\nabla \cdot u^{n+1} = 0 \quad \text{in } \Omega, \tag{2.15}$$

$$u^{n+1} \cdot \nu = 0 \quad \text{on } \partial\Omega, \tag{2.16}$$

where $g^{n+1} = \beta_0 \frac{1}{\triangle t} \tilde{u}^{n+1} + \nabla \overline{p}_l^{n+1}$. From now on we will consider (2.14)–(2.16).

3. PSEUDO-SPECTRAL DISCRETIZATION

To give a pseudo-spectral discretization of the Stokes systems we have to define spectral operators for the velocity and the pressure. This is done in the one-dimensional case first. In the two-dimensional case we get the corresponding operators by tensor product representation.

For $N \in \mathbb{N}$ let $\mathbb{P}_N$ be the space of polynomials of degree $\leq N$, while $\mathbb{P}_N^0$ is the space of polynomials in $\mathbb{P}_N$ which in addition fulfill the homogeneous Dirichlet boundary conditions. We approximate u by polynomials in $\mathbb{P}_N^0$ and p by polynomials in $\mathbb{P}_{N-1}$. We apply staggered grids where the velocity is defined at the Gauss–Lobatto nodes $(x_i, y_j) = (\cos \frac{i\pi}{N}, \cos \frac{j\pi}{N})$, $i, j = 0, \ldots, N$, while the pressure is evaluated at the Gauss nodes $(z_i, w_j) = (\cos \frac{(2i-1)\pi}{2N}, \cos \frac{(2j-1)\pi}{2N})$, $i, j = 1, \ldots, N$. We only consider even N. For odd N a similar treatment is possible.

Here we use the pseudo-spectral Chebyshev discretization. The corresponding spectral derivative operator for the velocity components can be found in [17].

After eliminating the boundary conditions we obtain

$$u'(x_j) \cong \left(\hat{D}_u^0 u\right)_j, \quad j = 0, \ldots, N,$$

where $\hat{D}_u^0 \in \mathbb{R}^{N+1,N-1}$, $x_j = \cos \frac{j\pi}{N}$, $j = 0, \ldots, N$. Now we have to interpolate between the Gauss–Lobatto and the Gauss nodes. If $T \in \mathbb{R}^{N,N+1}$ denotes the interpolation matrix we derive

$$u'(z_j) \cong \left(T\hat{D}_u^0 u\right)_j, \quad j = 1, \ldots, N.$$

The operator $D^0 = T\hat{D}_u^0 \in \mathbb{R}^{N,N-1}$ represents the first derivative operator. The second derivative is considered at the Gauss–Lobatto nodes and reads

$$u''(x_j) \cong \left(\left(D_u^2\right)^0 u\right)_j, \quad j = 1, \ldots, N-1,$$

where $(D_u^2)^0 \in \mathbb{R}^{N-1,N-1}$.

Now let us define the derivative operator for the pressure. Note that one has to interpolate between the Gauss and the Gauss–Lobatto nodes. We get

$$p'(x_j) \cong (Dp)_j, \quad j = 1, \ldots, N-1,$$

where $D \in \mathbb{R}^{N-1,N}$ is given by

$$D = T_{p_1} \hat{D}_p T_{p_2}.$$

$T_{p_2} \in \mathbb{R}^{N,N}$ interpolates into $\mathbb{P}_{N-1}$, $\hat{D}_p \in \mathbb{R}^{N,N}$ performs the differentiation in the coefficient space, and $T_{p_1} \in \mathbb{R}^{N-1,N}$ transforms back in the physical space. So we transform directly onto the Gauss–Lobatto nodes.

$\hat{D}_p = (d_{i,j})_{i,j=1,\dots,N}$ is explicitly defined as

$$d_{i,j} = \begin{cases} \frac{2(j-1)}{c_i}, & j = i+1, i+3, \dots, N-1 \\ 0, & \text{else} \end{cases}$$

$$c_i = \begin{cases} 2, & i = 1 \\ 1, & \text{else.} \end{cases}$$

For the two-dimensional space we calculate the derivative operators by the tensor product representation. We can introduce the partial differential operators for the velocity as

$$\frac{\partial}{\partial x} : D_x^0 = D^0 \otimes I, \quad \frac{\partial}{\partial y} : D_y^0 = I \otimes D^0,$$

$$\frac{\partial^2}{\partial x^2} : D_{xx}^0 = \left(D_u^2\right)^0 \otimes I, \quad \frac{\partial^2}{\partial y^2} : D_{yy}^0 = I \otimes \left(D_u^2\right)^0,$$

$$\frac{\partial^2}{\partial x^2} + \frac{\partial^2}{\partial y^2} : D_\triangle^0 = \left(D_{xx}^0 + D_{yy}^0\right),$$

where $I \in \mathbb{R}^{N,N}$ denotes the identity matrix. This induces: D_x^0, $D_y^0 \in \mathbb{R}^{N^2,(N-1)\cdot N}$.

For the pressure we work analogously to write

$$\frac{\partial}{\partial x} : D_x = D \otimes I, \quad \frac{\partial}{\partial y} : D_y = I \otimes D,$$

where D_x, $D_y \in \mathbb{R}^{(N-1)\cdot N,N^2}$.

Note that the transform from Gauss–Lobatto to Gauss nodes (and vice-versa) is done only in one variable. Therefore, we need a new definition for the pseudo-spectral discretization. For the velocity it is given by

$$\frac{\partial}{\partial x_G} : D_{x,G}^0 = D^0 \otimes T, \quad \frac{\partial}{\partial y_G} : D_{y,G}^0 = T \otimes D^0,$$

and for the pressure by

$$\frac{\partial}{\partial x_{GL}} : D_{x,GL} = D \otimes \left(T_{p_1} \cdot T_{p_2}\right), \quad \frac{\partial}{\partial y_{GL}} : D_{y,GL} = \left(T_{p_1} \cdot T_{p_2}\right) \otimes D.$$

The index G indicates that we transform onto the Gauss nodes (analogously, GL).

Now we are able to provide the pseudo-spectral discretization for the Stokes problem. First we consider (2.4)–(2.6), which gives

$$\left(-D_\triangle^0 + \beta_0 \frac{1}{\triangle t} I\right) u_1^{n+1} + D_{x,GL} p^{n+1} = \hat{f}_1^{n+1} \quad \text{in } \Omega, \tag{3.1}$$

$$\left(-D_\triangle^0 + \beta_0 \frac{1}{\triangle t} I\right) u_2^{n+1} + D_{y,GL} p^{n+1} = \hat{f}_2^{n+1} \quad \text{in } \Omega, \tag{3.2}$$

$$D^0_{x,G}u_1^{n+1} + D^0_{y,G}u_2^{n+1} = 0 \quad \text{in } \Omega, \tag{3.3}$$

$$u_1^{n+1} = u_2^{n+1} = 0 \quad \text{on } \partial\Omega, \tag{3.4}$$

where

$$\hat{f}_i^{n+1} = f_i^{n+1} - \frac{1}{\triangle t}\sum_{m=1}^{k}\beta_m u_i^{n+1-m} \quad (i = 1, 2).$$

Since we would like to use the operator splitting we have to solve a Helmholtz problem for the intermediate velocity components, which reads

$$\left(-D^0_{\triangle} + \beta_0\frac{1}{\triangle t}I\right)\tilde{u}_i^{n+1} = \tilde{f}_i^{n+1} \quad \text{in } \Omega, \tag{3.5}$$

$$\tilde{u}_i^{n+1} = 0 \quad \text{on } \partial\Omega, \quad i = 1, 2, \tag{3.6}$$

and

$$\beta_0\frac{1}{\triangle t}u_1^{n+1} + D_{x,GL}p^{n+1} = g_1^{n+1} \quad \text{in } \Omega, \tag{3.7}$$

$$\beta_0\frac{1}{\triangle t}u_2^{n+1} + D_{y,GL}p^{n+1} = g_2^{n+1} \quad \text{in } \Omega, \tag{3.8}$$

$$D^0_{x,G}u_1^{n+1} + D^0_{y,G}u_2^{n+1} = 0 \quad \text{in } \Omega, \tag{3.9}$$

$$u_1^{n+1} = u_2^{n+1} = 0 \quad \text{on } \partial\Omega. \tag{3.10}$$

By applying the divergence to the first two equations and further using the divergence-free condition (Uzawa decoupling) we finally obtain an equation with the pseudo-Laplacian for the pressure:

$$\left(D^0_{x,G}D_{x,GL} + D^0_{y,G}D_{y,GL}\right)p^{n+1} = D^0_{x,G}g_1^{n+1} + D^0_{y,G}g_2^{n+1}. \tag{3.11}$$

The operator $B \in \mathbb{R}^{N^2,N^2}$ with

$$\begin{aligned} B &= D^0_{x,G}D_{x,GL} + D^0_{y,G}D_{y,GL} \\ &= D^0_x D_x + D^0_y D_y \end{aligned}$$

is called the *pseudo-Laplacian* or *energy*.

4. PROPERTIES OF THE SPECTRAL PSEUDO-LAPLACIAN

In this section we consider the pseudo–Laplacian

$$B = D^0_x D_x + D^0_y D_y = A \otimes I + I \otimes A.$$

First, we consider the one-dimensional pseudo–Laplacian

$$A = D^0 D.$$

For an analysis of A we introduce a somewhat different representation of A. Let p be a polynomial in $\mathbb{P}_{N-1}$. Applying A to p is equivalent to first applying D to p and then D^0 to Dp. We obtain

$$p'(x_j) = (Dp)_j, \quad j = 1, \ldots, N-1,$$

where we consider p as a vector in $\mathbb{R}^N$.

Before applying D^0 to Dp we have to map p' onto a polynomial $p_0' \in \mathbb{P}_N^0$, which is defined by

$$p_0'(x_j) = p'(x_j), \quad j = 1, \ldots, N-1.$$

Obviously, p_0' can explicitly be written as

$$p_0' = p' + \alpha T_N' + \beta x T_N', \tag{4.1}$$

where T_N denotes the Nth Chebyshev polynomial. The coefficients α and β are determined such that $p_0'(1) = p_0'(-1) = 0$; i.e.,

$$\alpha = \frac{1}{2N^2}(p'(-1) - p'(1)),$$
$$\beta = -\frac{1}{2N^2}(p'(-1) + p'(1)).$$

Applying D^0 to Dp is equivalent to taking the first derivative of p_0'; i.e.,

$$p_0'' = p'' + \alpha T_N'' + \beta (x T_N')'. \tag{4.2}$$

We derive

$$\begin{aligned}
(Ap)_j &= p''(z_j) + \alpha T_N''(z_j) + \beta (x T_N')'(z_j) \\
&= p''(z_j) + \frac{1}{2N^2}(p'(-1) - p'(1)) T_N''(z_j) - \frac{1}{2N^2}(p'(-1) + p'(1)) \cdot (x T_N')'(z_j) \\
&= p''(z_j) + \frac{1}{2N^2} p'(-1) \cdot (T_N''(z_j) \cdot (1 - z_j) - T_N'(z_j)) \\
&\quad - \frac{1}{2N^2} p'(1)(T_N''(z_j) \cdot (1 + z_j) + T_N'(z_j)),
\end{aligned}$$

where z_j are the Gauss nodes for $j = 1, \ldots, N$.

Knowing that

$$T_N'(z_j) = (-1)^j \cdot N \cdot \frac{1}{\sqrt{1 - z_j^2}}$$

and

$$T_N''(z_j) = (-1)^j \cdot N \cdot \frac{z_j}{\left(1 - z_j^2\right)^{3/2}},$$

it follows for $(Ap)_j$, with $j = 1, \ldots, N$,

$$(Ap)_j = p''(z_j) + \frac{1}{2N} p'(-1) \frac{(-1)^{j+1}(1 - z_j)}{\left(1 - z_j^2\right)^{3/2}} + \frac{1}{2N} p'(1) \frac{(-1)^{j+1}(1 + z_j)}{\left(1 - z_j^2\right)^{3/2}}. \quad (4.3)$$

In order to represent A in matrix notation, we introduce two diagonal matrices D_-, $D_+ \in R^{N,N}$:

$$D_- = diag(d^-_{j,j})_{j=1,\ldots,N} : d^-_{j,j} = \frac{(-1)^{j+1}(1 - z_j)}{\left(1 - z_j^2\right)^{3/2}}, \quad j = 1, \ldots, N,$$

$$D_+ = diag(d^+_{j,j})_{j=1,\ldots,N} : d^+_{j,j} = \frac{(-1)^{j+1}(1 + z_j)}{\left(1 - z_j^2\right)^{3/2}}, \quad j = 1, \ldots, N.$$

Furthermore, we define two matrices P_+, $P_- \in R^{N,N}$ which represent $p'(1)$, $p'(-1)$. To be more precise

$$P_+ = e_+ f_+^t, \quad f_+ = e_+^t \hat{D}_p T_{p_2},$$
$$P_- = e_+ f_-^t, \quad f_- = e_-^t \hat{D}_p T_{p_2},$$

where $e_+ = (1, 1, \ldots, 1)^t, e_- = (1, -1, \ldots, 1, -1)^t \in \mathbb{R}^N$. Obviously P_+ and P_- have rank 1. We obtain the following representation:

$$A = D^2 + D_- P_- + D_+ P_+. \quad (4.4)$$

Our aim is to prove that the eigenvalues of A are real.

Let $p \in \mathbb{P}_{N-1}$ be an eigenfunction of A with respect to the eigenvalue λ. We have

$$p'' + \alpha T_N'' + \beta (x T_N')' - \lambda p \equiv 0. \quad (4.5)$$

First, we consider the case $\lambda = 0$. It is easy to see that $p = const. \neq 0$ is an eigenfuction. Furthermore, notice that $p'' \in \mathbb{P}_{N-3}$ but $\alpha T_N'' + \beta (x T_n')' \in \mathbb{P}_{N-1}$. This implies $\alpha = \beta = 0$, inducing

$$p'(-1) = p'(1) = 0.$$

This implies that all eigenfunctions associated with $\lambda = 0$ are constant.

In what follows we consider the case $\lambda \neq 0$, $p \neq const.$ Let us introduce $p_1 \equiv p_1(x, \lambda) \in \mathbb{P}_{N-2}$, $p_2 \equiv p_2(x, \lambda) \in \mathbb{P}_{N-1}$ satisfying

$$\lambda p_1 - p_1'' = T_N'',$$
$$\lambda p_2 - p_2'' = (x T_N')'.$$

We define p_1 and p_2 by

$$p_1 = \sum_{k=0}^{\infty} \lambda^{-k-1} \frac{\partial^{2k}}{\partial x^{2k}} T_N'',$$

$$p_2 = \sum_{k=0}^{\infty} \lambda^{-k-1} \frac{\partial^{2k}}{\partial x^{2k}} (x T_N')'$$

(see [11]), and p is given by

$$p = \alpha p_1 + \beta p_2.$$

Here α, β have to be chosen such that

$$\begin{aligned}(p_1'(1,\lambda) + T_N'(1)) \cdot \alpha + (p_2'(1,\lambda) + T_N'(1)) \cdot \beta = 0,\\ (p_1'(-1,\lambda) + T_N'(-1)) \cdot \alpha + (p_2'(-1,\lambda) - T_N'(-1)) \cdot \beta = 0.\end{aligned}$$

This system of equations has a nontrivial solution if and only if the determinant vanishes, i.e.,

$$\begin{aligned}[(p_1'(1,\lambda) + T_N'(1))(-p_2'(-1,\lambda) + T_N'(-1))] - [(p_1'(-1,\lambda)\\ + T_N'(-1))(p_2'(1,\lambda) + T_N'(1))] = 0.\end{aligned} \tag{4.6}$$

By using

$$p_1'(-1,\lambda) = -p_1'(1,\lambda) \quad \text{and} \quad p_2'(-1,\lambda) = p_2'(1,\lambda)$$

and $T_N'(-1) = -T_N'(1) = -N^2$ we finally arrive at the following two characteristic equations:

$$\begin{aligned}p_1'(1,\lambda) + N^2 = 0,\\ p_2'(1,\lambda) + N^2 = 0.\end{aligned}$$

These equations determine $(N-1)$ nonzero eigenvalues since p_1' and p_2' are both polynomials of degree $\frac{N}{2}$ in λ^{-1}.

For instance, for $N = 4$ we obtain the two characteristic equations

$$192 \cdot \lambda^{-1} + 16 = 0, \quad 768 \cdot \lambda^{-2} + 352\lambda^{-1} + 16 = 0,$$

which give the three eigenvalues $\lambda_1 = 12$, $\lambda_{2,3} = -11 \pm \sqrt{73}$ (see also Table I).

Let us introduce

$$f_N(x,\mu) = \sum_{k=0}^{\infty} \mu^k \frac{\partial^{k+1}}{\partial x^{k+1}} T_N(x) \tag{4.7}$$

and

$$g_N(x,\mu) = \sum_{k=0}^{\infty} \mu^{k+1} \frac{\partial^k}{\partial x^k} (xT_N')'(x) + xT_N'(x). \tag{4.8}$$

Now we prove that the roots of f_N and g_N have negative real parts.

LEMMA 4.1. *Let f_N and g_N be defined as in* (4.7) *and* (4.8). *Then $f_N(1, \mu)$ and $g_N(1, \mu)$ are Hurwitz polynomials.*

Proof. The proof for f_N has already been given in [11]. Here we only consider g_N. We easily obtain

$$g_N(x, \mu) - \mu \frac{\partial}{\partial x} g_N(x, \mu) = x T_N'(x).$$

Let $w_N(t, \mu) = e^{(1/\mu)t} g_N(x, \mu)$. Then

$$\frac{\partial w_N}{\partial t} - \frac{\partial w_N}{\partial x} = \frac{1}{\mu} \cdot e^{(1/\mu)t} \cdot x T_N'(x),$$

and if μ is a root of $g_N(1, \mu)$ then μ is also a root of w_N, i.e.,

$$w_N(1, t) = 0.$$

Furthermore we know that

$$\frac{1}{\mu} \cdot e^{(1/\mu)t} \cdot x_j T_N'(x_j) = 0, \quad j = 1, \ldots, N-1,$$

where x_j denote the Chebyshev Gauss–Lobatto nodes. Now it can be shown (see [11]) that $w_N(x, t)$ decreases in time and therefore Re $\mu < 0$. ∎

Now let

$$f_N^1(\mu) = \sum_{k=0}^{\infty} \mu^{k+1} \frac{\partial^{2k+3}}{\partial x^{2k+3}} T_N(1) + T_N'(1), \tag{4.9}$$

$$f_N^2(\mu) = \sum_{k=0}^{\infty} \mu^{k} \frac{\partial^{2k+2}}{\partial x^{2k+2}} T_N(1) \tag{4.10}$$

and

$$g_N^1(\mu) = \sum_{k=0}^{\infty} \mu^{k+1} \frac{\partial^{2k+1}}{\partial x^{2k+1}} (x T_N')'(1) + (x T_N')(1), \tag{4.11}$$

$$g_N^2(\mu) = \sum_{k=0}^{\infty} \mu^{k} \frac{\partial^{2k}}{\partial x^{2k}} (x T_N')'(1). \tag{4.12}$$

LEMMA 4.2. *Let f_N^1, f_N^2, g_N^1, and g_N^2 be defined as in* (4.9)–(4.12). *Then f_N^1 and f_N^2, g_N^1 and g_N^2 form a positive pair.*

Proof. One easily checks that

$$f_N^1(\mu^2) + \mu \cdot f_N^2(\mu^2) = f_N(1, \mu),$$
$$g_N^1(\mu^2) + \mu \cdot g_N^2(\mu^2) = g_N(1, \mu),$$

where f_N and g_N are Hurwitz polynomials (see Lemma 4.1). This concludes the proof. ∎

By means of this lemma we immediately obtain the following theorem.

TABLE I
λ_{min} and λ_{max} of A

N	λ_{min}	λ_{max}	λ_{max}/N^3
4	2.4560	$1.9544 \cdot 10^1$	0.3054
8	2.4674	$2.1437 \cdot 10^2$	0.4187
16	2.4674	$3.1748 \cdot 10^3$	0.7751
32	2.4674	$4.9939 \cdot 10^4$	1.5240
64	2.4674	$7.9573 \cdot 10^5$	3.0355
128	2.4674	$1.2719 \cdot 10^7$	6.0649

THEOREM 4.1. *The eigenvalues of the spectral operator A are real. One eigenvalue is equal to zero and the remaining $N-1$ eigenvalues are all distinct and have negative sign. Also, the eigenvalues of the spectral operator B are real. One eigenvalue is equal to zero and the remaining N^2-1 eigenvalues have negative sign.*

Proof. Let $\mu = \lambda^{-1}$, which induces

$$f_N^1(\lambda^{-1}) = p_1'(1,\lambda) + N^2 \quad \text{and} \quad g_N^1(\lambda^{-1}) = p_2'(1,\lambda) + N^2.$$

We see that f_N^1 and g_N^1 are identical to the characteristic polynomials. By using Lemma 4.2 we obtain the desired results of our theorem for the one-dimensional pseudo–Laplacian.

The properties of the spectral operator B directly results form the tensor representation with A. In [14], Theorem 4.4, it is shown that if $\lambda, \mu \in \sigma(A)$ then $\lambda + \mu$ is an eigenvalue of the Kronecker sum $(A \otimes I) + (I \otimes A) = B$. ■

REMARK 4.1. *The result of Theorem* (4.1) *implicitly indicates that our discretization does not introduce spurious modes.*

We have calculated the eigenvalues of A and B numerically using the QR-Algorithm (see e.g. [9]). All calculations were done on a Sun Ultra Enterprise 2000 under Solaris 2.6. We define

$$\lambda_{min} = \min\{|\lambda| \mid \lambda \neq 0 \text{ eigenvalue of } A\},$$
$$\lambda_{max} = \max\{|\lambda| \mid \lambda \neq 0 \text{ eigenvalue of } A\}.$$

In Table I we present the maximal and the minimal eigenvalues λ_{min} and λ_{max} of A. It is numerically shown that λ_{min} and λ_{max} of A have a similar behavior as the eigenvalues of $(D^2)^0$. For increasing N the minimal eigenvalue λ_{min} approximates $\pi^2/4$.

Table II presents λ_{min} and λ_{max} for the two-dimensional operator B.

TABLE II
λ_{min} and λ_{max} of B

N	λ_{min}	λ_{max}	λ_{max}/N^3
4	2.4560	$3.9088 \cdot 10^1$	0.6108
8	2.4674	$4.2874 \cdot 10^2$	0.8374
16	2.4674	$6.3496 \cdot 10^3$	1.5502

5. PRECONDITIONING

In the following section, efficient FD preconditioners for the spectral operator are presented.

5.1. *The One-Dimensional Case*

To give a FD preconditioner for A we make use of the representations in (4.3) and (4.4). First, we have to find approximations for

$$p''(z_j), \quad j = 1, \ldots, N, \, p'(-1), \text{ and } p'(1).$$

For $p''(z_j)$, $j = 2, \ldots, N-1$, we use the standard central FD scheme, i.e.,

$$p''(z_j) \cong 2 \cdot \left(\frac{p(z_{j+1}) - p(z_j)}{z_{j+1} - z_j} - \frac{p(z_j) - p(z_{j-1})}{z_j - z_{j-1}} \right) \cdot \frac{1}{z_{j+1} - z_{j-1}}. \tag{5.1}$$

One observes that (5.1) is equivalent to

$$p''(z_j) \cong a_j \, p(z_{j-1}) - (a_j + c_j) p(z_j) + c_j \, p(z_{j+1}), \tag{5.2}$$

where

$$a_j = \frac{\alpha}{s_{j-1} s_{j-\frac{1}{2}}}, \quad c_j = \frac{\alpha}{s_j s_{j-\frac{1}{2}}}$$

and

$$\alpha = \frac{1}{2 s_{\frac{1}{2}} s_1}, \quad s_j = \sin\left(\frac{j\pi}{N} \right).$$

First, we try to apply one-sided first-order approximations for $p''(z_1)$ and $p''(z_N)$, i.e.,

$$p''(z_1) \cong a_2 p(z_1) - (a_2 + c_2) p(z_2) + c_2 p(z_3), \tag{5.3}$$

$$p''(z_N) \cong a_{N-1} p(z_{N-2}) - (a_{N-1} + c_{N-1}) p(z_{N-1}) + c_{N-1} p(z_N). \tag{5.4}$$

For $p'(-1)$ and $p'(1)$ we also use one-sided finite differences and obtain

$$\begin{aligned} p'(1) &\cong \frac{1}{z_1 - z_2} \cdot (p(z_1) - p(z_2)) \\ &= \frac{1}{2 s_1 s_{\frac{1}{2}}} (p(z_1) - p(z_2)) \end{aligned} \tag{5.5}$$

and

$$\begin{aligned} p'(-1) &\cong \frac{1}{z_N - z_{N-1}} \cdot (p(z_N) - p(z_{N-1})) \\ &= -\frac{1}{2 s_1 s_{\frac{1}{2}}} (p(z_N) - p(z_{N-1})). \end{aligned} \tag{5.6}$$

The FD scheme (5.2)–(5.6) is now associated with an FD operator, here called A^1_{FD}.

We want to examine the preconditioning properties of $A^1_{FD,0}$. $c = const. \neq 0$ is obviously an eigenfunction of A^1_{FD} with eigenvalue zero. To check the properties of A^1_{FD} we have to eliminate the constant mode. To achieve this, we introduce a transformation matrix E, which is defined by

$$p = Eq,$$

where

$$E = \begin{pmatrix} 1 & 0 & 0 & \cdots & 0 & 0 & 1 \\ 0 & 1 & 0 & \cdots & 0 & 0 & 1 \\ 0 & 0 & 1 & \cdots & 0 & 0 & 1 \\ & \vdots & & \cdots & & \vdots & \\ 0 & 0 & 0 & \cdots & 1 & 0 & 1 \\ 0 & 0 & 0 & \cdots & 0 & 1 & 1 \\ 0 & 0 & 0 & \cdots & 0 & 0 & 1 \end{pmatrix}.$$

We now solve the problem in q and consider the modified operators

$$\hat{A} = AE, \quad \hat{A}^1_{FD} = A^1_{FD}E.$$

One can see that $\hat{A}$ and $\hat{A}^1_{FD}$ are identical to A and A^1_{FD}, apart from the last column which is now identical to zero since the last column corresponds to constants. Matrix E can easily be inverted and does not change the structure of the spectral operator. By eliminating the last column and one of the rows (here it is also the last one) we get a nonsingular system in $\mathbb{R}^{N-1,N-1}$. The corresponding spectral or FD operators are called

$$\hat{A}_0 \in \mathbb{R}^{N-1,N-1}, \quad \hat{A}^1_{FD,0} \in \mathbb{R}^{N-1,N-1}.$$

Table III contains the eigenvalues of $(\hat{A}^1_{FD,0})^{-1}\hat{A}_0$. We numerically observe that all eigenvalues are real.

One can see that the approximation of first order is a good preconditioner. The minimal eigenvalue is 1 and the maximal eigenvalue approximates $\pi^2/4$, independent of N.

Now we want to use finite differences of second order for approximating $p''(z_1)$, $p''(z_N)$, $p'(1)$, and $p'(-1)$. The corresponding FD operator is called $\hat{A}^2_{FD,0}$ and the eigenvalues of $(\hat{A}^2_{FD,0})^{-1}\hat{A}_0$ are presented in Table IV. Again we numerically obtain real eigenvalues and the minimal eigenvalue is 1. We also see that the maximal eigenvalue

TABLE III
λ_{min} and λ_{max} of $(\hat{A}^1_{FD,0})^{-1}\hat{A}_0$

N	λ_{min}	λ_{max}
4	1.00	1.359246
8	1.00	1.966774
16	1.00	2.246328
32	1.00	2.367677
64	1.00	2.421208
128	1.00	2.445527

TABLE IV
λ_{min} and λ_{max} of $(\hat{A}^2_{FD,0})^{-1}\hat{A}_0$

N	λ_{min}	λ_{max}
4	1.00	1.295264
8	1.00	1.970879
16	1.00	2.249901
32	1.00	2.369083
64	1.00	2.421703
128	1.00	2.445697

approximates $\pi^2/4$. So this approximation yields no advantage compared with our first approximation.

Figures 1 and 2 present a graphical comparison between the method in [12] ($N,N-2$ method) and the method just presented. In relation to these approximations our method has better properties than the $N,N-2$ method. Finally, we employ the spectral scheme for the derivatives $p''(z_1)$, $p''(z_N)$, $p'(1)$, and $p'(-1)$. Because of the corresponding FD operator $\hat{A}^{sp}_{FD,0} \in \mathbb{R}^{N-1,-1}$ we especially use the presentation of (4.4). From Table V it can be seen that the maximal eigenvalue from $(\hat{A}^{sp}_{FD,0})^{-1}\hat{A}_0$ is bounded independent of N.

Figure 3 shows that in the case of the spectral scheme our method with staggered grids does not have preconditioner properties comparable to those of the $N,N-2$ method. But the maximal eigenvalue is also bounded independent of N.

At last we consider the case that $p'(-1)$ and $p'(1)$ are both equal to zero. We obtain the Neumann condition

$$p'(-1) = p'(1) = 0.$$

By using this boundary condition the FD approximations for $p''(z_1)$ and $p''(z_N)$ now read as follows:

$$p''(z_1) \cong -(a_1 + c_1)p(z_1) + (a_1 + c_1)p(z_2),$$
$$p''(z_N) \cong -(a_{N-1} + c_{N-1})p(z_{N-1}) + (a_{N-1} + c_{N-1})p(z_{N-2}).$$

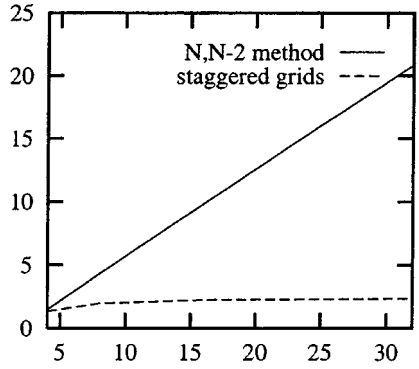

FIG. 1. Maximal eigenvalue of preconditioner $(\hat{A}^1_{FD,0})^{-1}\hat{A}_0$.

TABLE V
λ_{min} and λ_{max} of $(\hat{A}^{sp}_{FD,0})^{-1}\hat{A}_0$

N	λ_{min}	λ_{max}
4	1.00	1.276142
8	1.00	2.228686
16	1.00	3.114336
32	1.00	3.761935
64	1.00	4.167232
128	1.00	4.396862

TABLE VI
λ_{min} and λ_{max} of $(\hat{A}^{NE}_{FD,0})^{-1}\hat{A}_0$

N	λ_{min}	λ_{max}
4	1.121320	1.971857
8	1.019224	2.533468
16	1.003583	2.663229
32	1.000716	2.688467
64	1.000149	2.692843
128	1.000032	2.693627

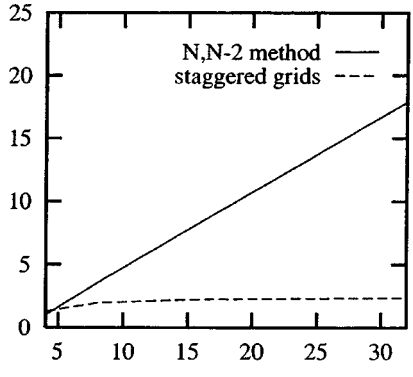

FIG. 2. Maximal eigenvalue of preconditioner $(\hat{A}^2_{FD,0})^{-1}\hat{A}_0$.

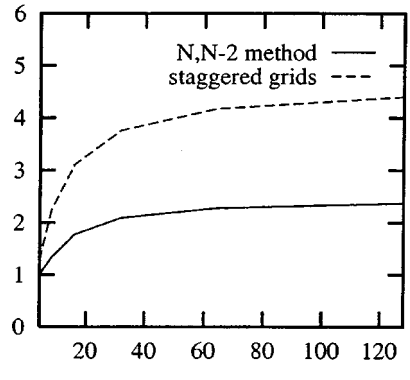

FIG. 3. Maximal eigenvalue of preconditioner $(\hat{A}^{sp}_{FD,0})^{-1}\hat{A}_0$.

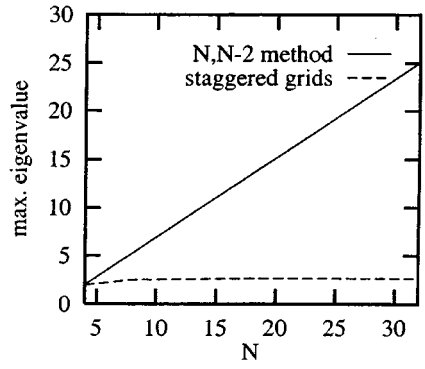

FIG. 4. Maximal eigenvalue of preconditioner $(\hat{A}^{NE}_{FD,0})^{-1}\hat{A}_0$.

The corresponding FD operator is called $\hat{A}^{NE}_{FD,0}$. Figure 4 shows that the maximal eigenvalue of $(\hat{A}^{NE}_{FD,0})^{-1}\hat{A}_0$ is bounded independent of N (see also Table VI).

Because $\hat{A}^{NE}_{FD,0}$ is a tridiagonal matrix, this preconditioner is preferred in practice. This is the only preconditioner which guarantees that the eigenvalues of the preconditioned operator all remain of the same sign. In the case of the $N,N-2$-method we also tested $\hat{A}^{NE}_{FD,0}$ as a preconditioner in practice, but we observed that the maximal eigenvalue behaves as $O(N)$.

5.2. *The Two-Dimensional Case*

Similar results can be obtained in the two-dimensional case. Here we only consider the two-dimensional operator for A^1_{FD} and A^{sp}_{FD}, which can be constructed analogously to the spectral operators by means of tensor products.

Let

$$\hat{B} = B(E \otimes E)$$

and

$$\hat{B}^1_{FD} = \hat{A}^1_{FD} \otimes E + E \otimes \hat{A}^1_{FD},$$
$$\hat{B}^{sp}_{FD} = \hat{A}^{sp}_{FD} \otimes E + E \otimes \hat{A}^{sp}_{FD}.$$

The operators $\hat{B}_0$, $\hat{B}^1_{FD,0}$, and $\hat{B}^{sp}_{FD,0}$ are obtained by eliminating the last column and the last row. One can extract the eigenvalues of $(\hat{B}^1_{FD,0})^{-1}\hat{B}_0$ and $(\hat{B}^{sp}_{FD,0})^{-1}\hat{B}_0$ from Tables VII

TABLE VII
λ_{min} and λ_{max} of $(\hat{B}^1_{FD,0})^{-1}\hat{B}_0$

N	λ_{min}	λ_{max}
4	1.00	5.425331
8	1.00	3.175775
16	1.00	2.706077

TABLE VIII
λ_{min} and λ_{max} of $(\hat{B}^{sp}_{FD,0})^{-1}\hat{B}_0$

N	λ_{min}	λ_{max}
4	0.929963	1.276142
8	0.799335	2.228690
16	0.732044	3.114336

and VIII. By approximation with FD differences of the first order one can see that the maximal eigenvalue of $(\hat{B}^1_{FD,0})^{-1}\hat{B}_0$ approximates the maximal eigenvalue of $(\hat{A}^1_{FD,0})^{-1}\hat{A}_0$.

In the case of the spectral scheme we obtain complex eigenvalues and the minimal eigenvalue is less than one. The maximal eigenvalue is close to the maximal eigenvalue of $(\hat{A}^{sp}_{FD,0})^{-1}\hat{A}_0$.

6. NUMERICAL RESULTS FOR THE STOKES EQUATIONS

6.1. *The Steady Case*

First, we give an example for the solution of (2.1)–(2.3). Let

$$\bar{x} = \frac{1}{2}(x+1), \quad \bar{y} = \frac{1}{2}(y+1).$$

Because $x, y \in [-1, 1]$ we know that $\bar{x}, \bar{y} \in [0, 1]$.

Let us define

$$u_1(x, y) = r(\bar{x})s(\bar{y}), \quad u_2(x, y) = -s(\bar{x})r(\bar{y}),$$
$$p(x, y) = \exp(\bar{x} + \bar{y} - 1),$$

where

$$r(\bar{x}) = \bar{x}^2(1-\bar{x})^2,$$
$$s(\bar{y}) = 2\bar{y}(1-\bar{y})^2 - 2\bar{y}^2(1-\bar{y}).$$

Hence the functions u_1, u_2 satisfy

$$u_1(x, y) = u_2(x, y) = 0 \quad \text{for } (x, y) \in \partial\Omega.$$

Furthermore, r and s are choosen such that $r' = s$, which leads us to

$$\frac{\partial}{\partial x}u_1(x, y) + \frac{\partial}{\partial y}u_2(x, y) = \frac{1}{2}(r'(\bar{x})s(\bar{y}) - s(\bar{x})r'(\bar{y})) = 0.$$

Therefore, the velocity field is divergence-free. By substitution of u_1, u_2 in (2.1) we obtain the right-hand side f.

Let v_1^N, v_2^N, and q^N be the approximations of u_1, u_2, and p. Then we can calculate the absolute errors

$$ERU1 = \left\|u_1 - v_1^N\right\|_2, \quad ERU2 = \left\|u_2 - v_2^N\right\|_2, \quad ERP = \|p - q^N\|_2,$$

TABLE IX
Results for the Velocity and the Pseudo–Laplacian

N	$ERU1 = ERU2$	ERP
4	$4.686 \cdot 10^{-6}$	$2.355 \cdot 10^{-2}$
8	$3.678 \cdot 10^{-12}$	$3.807 \cdot 10^{-3}$
12	$3.555 \cdot 10^{-12}$	$1.204 \cdot 10^{-3}$

where

$$\|v\|_2 = \left[\sum_{i,j=0}^{N} v(x_i, y_j)^2\right]^{\frac{1}{2}} \Big/ N, \; \|q\|_2 = \left[\sum_{i,j=1}^{N} p(z_i, w_j)^2\right]^{\frac{1}{2}} \Big/ N$$

denote the discrete L^2-norms in Ω.

We calculate the above errors by taking sufficient time steps until the stopping criterion,

$$\|u^n - u^{n+1}\|_2 \leq 1.0 \cdot 10^{-14},$$

is satisfied.

Table IX presents the results for the pseudo–Laplacian by using order-one methods for the time discretization and the extrapolation of p. Obviously, the accuracy obtained in p is much worse than that of u. This is because for the approximation of the pressure we use polynomials of one degree less than that for the velocity by the use of staggered grids. This means that more weight is put into approximating the velocity (compared to [12]). In particular the larger test space guarantees that (2.2) is satisfied more accurately.

6.2. *The Unsteady Case*

If v^{n+1} is the exact velocity and q^{n+1} the exact pressure at the time level t_{n+1}, we obtain from (2.9) that

$$\frac{\beta_0}{\triangle t}(u^{n+1} - v^{n+1} + v^{n+1} - \tilde{u}^{n+1}) = \nabla\left(q^{n+1} - p^{n+1} + \overline{p}_l^{n+1} - q^{n+1}\right) \quad \text{in } \Omega.$$

Since the intermediate velocity $\tilde{u}^{n+1}$ is determined by a k-th order time differentiation scheme and the extrapolated pressure by a l-th order scheme we observe that the error function

$$u^{n+1} - v^{n+1} + \frac{\triangle t}{\beta_0}\nabla(p^{n+1} - q^{n+1}) \tag{6.1}$$

behaves as

$$O(\triangle t^k) + O(\triangle t^{l+1}).$$

By taking $r = k = l + 1$ we finally find out that (6.1) behaves as $O(\triangle t^r)$ for $\triangle t \to 0$.

By combining a backward Euler scheme of second order with a first-order extrapolation we obtain a method which is completely of second order in time. This theoretical result

TABLE X
Results for the Velocity and the Pseudo–Laplacian for $N = 12$ and $r = 2$

$\triangle t$	E_{u_1}	Ratio	E_{u_2}	Ratio	E_p	Ratio
$\frac{1}{32}$	$9.818 \cdot 10^{-4}$		$1.053 \cdot 10^{-3}$		$5.831 \cdot 10^{-2}$	
$\frac{1}{64}$	$2.513 \cdot 10^{-4}$	3.907	$2.696 \cdot 10^{-4}$	3.906	$2.666 \cdot 10^{-2}$	2.187
$\frac{1}{128}$	$6.333 \cdot 10^{-5}$	3.968	$6.796 \cdot 10^{-5}$	3.967	$9.617 \cdot 10^{-3}$	2.564
$\frac{1}{256}$	$1.584 \cdot 10^{-5}$	3.998	$1.700 \cdot 10^{-5}$	3.998	$4.800 \cdot 10^{-3}$	2.004

is also confirmed by numerical calculations. For that purpose we consider the following example on $[0, 1]^2$. Let

$$\begin{aligned} u_1(x, y, t) &= z(t)r(\bar{x})s(\bar{y}), \\ u_2(x, y, t) &= -z(t)s(\bar{x})r(\bar{y}), \\ p(x, y, t) &= w(t)\exp(\bar{x} + \bar{y} - 1), \end{aligned}$$

where

$$\begin{aligned} r(\bar{x}) &= \sin(\pi\bar{x})^2, \\ s(\bar{x}) &= r'(\bar{x}), \\ z(t) &= (2\pi - 1 + \sin(2\pi t)) \cdot \frac{1}{2\pi}, \\ w(t) &= \cos(2\pi t). \end{aligned}$$

We calculate the mean quadratic errors:

$$\begin{aligned} E_{u1} &= \max\{ERU1 : t \geq 0\}, \\ E_{u2} &= \max\{ERU2 : t \geq 0\}, \\ E_p &= \max\{ERP : t \geq 0\}. \end{aligned}$$

We compute these errors after the effect of initialization has disappeared. Then the errors become periodic in time because our functions z and w' are periodic. The numerical results for the case $N = 12$ and $\triangle t = \frac{1}{32}, \frac{1}{64}, \frac{1}{128}$, and $\frac{1}{256}$ are given in Table X for $r = 2$.

For $r = 3$ this method does not converge because of the use of staggered grids. Therefore, we give also the numerical results for the case $k = 1$ and $l = 1$ (see Table XI).

TABLE XI
Results for the Pseudo–Laplacian for $N = 12$ and $k = l = 1$

$\triangle t$	E_{u_1}	Ratio	E_{u_2}	Ratio	E_p	Ratio
$\frac{1}{32}$	$6.477 \cdot 10^{-3}$		$6.658 \cdot 10^{-3}$		$7.024 \cdot 10^{-2}$	
$\frac{1}{64}$	$3.268 \cdot 10^{-3}$	1.982	$3.313 \cdot 10^{-3}$	2.010	$3.111 \cdot 10^{-2}$	2.258
$\frac{1}{128}$	$1.647 \cdot 10^{-3}$	1.984	$1.659 \cdot 10^{-3}$	1.997	$1.195 \cdot 10^{-2}$	2.603
$\frac{1}{256}$	$8.281 \cdot 10^{-4}$	1.989	$8.310 \cdot 10^{-4}$	1.996	$4.873 \cdot 10^{-3}$	2.454

7. THE NAVIER–STOKES EQUATIONS

Now we consider the unsteady Navier–Stokes equations for incompressible flows in velocity–pressure formulation:

$$\frac{\partial u}{\partial t} - \frac{1}{\mathrm{Re}}\nabla^2 u + \nabla p + (u \cdot \nabla)u = f \quad \text{in } \Omega =]-1, 1[^2, \tag{7.1}$$

$$\nabla \cdot u = 0 \quad \text{in } \Omega =]-1, 1[^2, \tag{7.2}$$

$$u = h \quad \text{on } \partial\Omega, \tag{7.3}$$

$$u = u_0 \quad \text{for } t = 0, \text{ in } \Omega =]-1, 1[^2. \tag{7.4}$$

As in (2.7)–(2.11) we obtain

$$L^n_{t,2}\tilde{u}^{n+1} - \frac{1}{\mathrm{Re}}\nabla^2\tilde{u}^{n+1} + 2 \cdot (u^n \cdot \nabla)u^n - (u^{n-1} \cdot \nabla)u^{n-1} + \nabla \overline{p}_1^{n+1} = f^{n+1} \quad \text{in } \Omega, \tag{7.5}$$

$$\tilde{u}^{n+1}_{|\partial\Omega} = h^{n+1}, \tag{7.6}$$

and

$$\frac{3}{2} \cdot \frac{u^{n+1} - \tilde{u}^{n+1}}{\triangle t} + \nabla\left(p^{n+1} - \overline{p}_1^{n+1}\right) = 0 \quad \text{in } \Omega, \tag{7.7}$$

$$\nabla \cdot u^{n+1} = 0 \quad \text{in } \Omega, \tag{7.8}$$

$$u^{n+1} \cdot \nu_{|\partial\Omega} = h^{n+1} \cdot \nu. \tag{7.9}$$

For the approximation of the convective term we use the Adams–Bashforth scheme of second order. We consider the following example:

$$u_1(x, y, t) = \cos(\gamma t) \cdot \sin\left(\frac{\pi x}{2}\right) \cdot \cos\left(\frac{\pi y}{2}\right),$$

$$u_2(x, y, t) = -\cos(\gamma t) \cdot \cos\left(\frac{\pi x}{2}\right) \cdot \sin\left(\frac{\pi y}{2}\right),$$

$$p(x, y, t) = \frac{1}{4} \cdot \cos^2(\gamma t)(\cos(\pi x) + \cos(\pi y)) + 10(x + y) \cdot \cos(\gamma t).$$

Obviously, u_1 and u_2 satisfy $\nabla \cdot u = 0$:

$$\frac{\partial u_1}{\partial x} + \frac{\partial u_2}{\partial y} = \frac{\pi}{2} \cdot \cos(\gamma t) \cdot \cos\left(\frac{\pi x}{2}\right) \cdot \cos\left(\frac{\pi y}{2}\right) - \frac{\pi}{2} \cdot \cos(\gamma t) \cdot \cos\left(\frac{\pi x}{2}\right) \cdot \cos\left(\frac{\pi y}{2}\right) = 0.$$

The source term f is defined by (7.1), h by (7.3), and the initial condition u_0 by (7.4). The Reynolds number is $\mathrm{Re} = 100$ and to start the time-integration the fields at levels $-2\triangle t$, $-\triangle t$, and 0 are equal to the exact solution.

7.1. *The Steady Case*

First we consider the steady case; i.e., $\gamma = 0$. We compute the error

$$I_\phi = \|\phi_N - \phi\|_I,$$

TABLE XII
Results for the Navier–Stokes Equations

N	I_{u_1}	I_{u_2}	I_p
8	$2.856 \cdot 10^{-7}$	$2.720 \cdot 10^{-7}$	$6.350 \cdot 10^{-6}$
12	$5.840 \cdot 10^{-12}$	$4.780 \cdot 10^{-12}$	$1.075 \cdot 10^{-9}$
16	$1.087 \cdot 10^{-14}$	$1.172 \cdot 10^{-14}$	$2.105 \cdot 10^{-13}$

i.e., the discrete error at the inner collocation points, where

$$\|\phi\|_I^2 = \frac{1}{(N-1)^2} \cdot \sum_{i,j=1}^{N-1} \phi(x_i, y_j)^2.$$

Table XII contains the results for $\triangle t = 0.01$ and $N = 8$, 12, and 16.

From Table XIII we can see that we achieved a second-order method in time for u.

7.2. *The Unsteady Case*

For the unsteady case we choose $\gamma = 5$, $\triangle t = 0.001$, and $N = 16$. Figure 5 demonstrates the temporal evolution of the errors E_{u1} and E_p. We observe no amplification of the oscillatiing errors in time, expressing the stability of the numerical solution.

7.3 *The Regularized Cavity Flow*

Finally, the regularized cavity flow in the domain $0 \le \bar{x}, \bar{y} \le 1$ is computed. On the edge $\bar{y} = 1$ the fluid velocity is

$$u_1(\bar{x}, 1) = -16\bar{x}^2(1-\bar{x})^2,$$
$$u_2(\bar{x}, 1) = 0,$$

where $u_1 = u_2 = 0$ on the other three edges. The source term f is identical to zero.

To compare our results with the results in [4] we have to determine the streamfunction ψ and the vorticity ω. There we have to compute in each time step

$$\omega^{n+1} = \frac{\partial u_2^{n+1}}{\partial \bar{x}} - \frac{\partial u_1^{n+1}}{\partial \bar{y}}.$$

TABLE XIII
Results for the Navier–Stokes Equations for $N = 12$ and $r = 2$, $\gamma = 5$

$\triangle t$	I_{u_1}	Ratio	I_{u_2}	Ratio	I_p	Ratio
$\frac{1}{32}$	$1.6021 \cdot 10^{-2}$		$1.6021 \cdot 10^{-2}$		$5.520 \cdot 10^{-2}$	
$\frac{1}{64}$	$3.4444 \cdot 10^{-3}$	4.6513	$3.4444 \cdot 10^{-3}$	4.6513	$1.2652 \cdot 10^{-2}$	4.3629
$\frac{1}{128}$	$8.2226 \cdot 10^{-4}$	4.1889	$8.2245 \cdot 10^{-4}$	4.1880	$3.0681 \cdot 10^{-3}$	4.1237
$\frac{1}{256}$	$2.0133 \cdot 10^{-4}$	4.0841	$2.0120 \cdot 10^{-4}$	4.0877	$7.6495 \cdot 10^{-4}$	4.0108

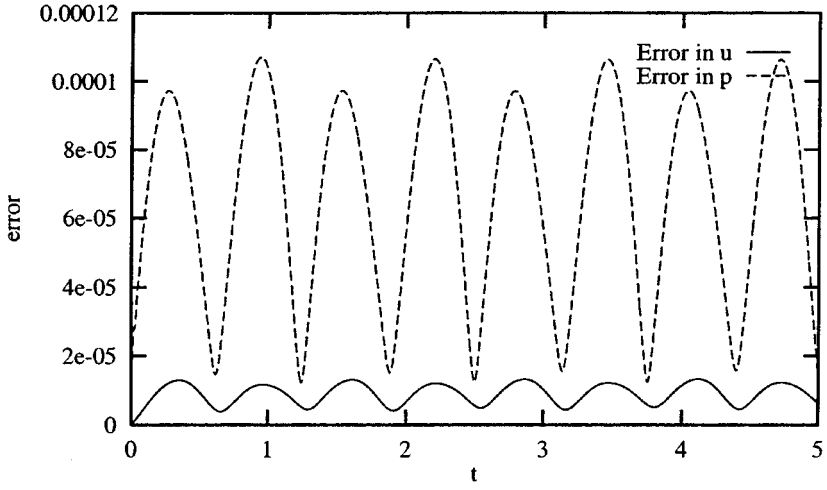

FIG. 5. Temporal evolution of the errors E_{u_1} and E_p for $\triangle t = 0.001$ and $N = 16$.

We consider that the steady case is reached when

$$\frac{\max_{i,j}\left|\omega_{i,j}^{n+1} - \omega_{i,j}^{n}\right|}{\triangle t \cdot \max_{i,j}\left|\omega_{i,j}^{n+1}\right|} \leq 2 \cdot 10^{-6}. \tag{7.10}$$

Then we calculate the streamfunction ψ by

$$\nabla^2 \psi = -\omega \quad \text{in } \Omega =]0, 1[^2. \tag{7.11}$$

Table XIV displays the maximal time step $\triangle t_c$ for $N = 16, 20$, and 24 for Reynolds numbers $\mathrm{Re} = 100$ and 400. Table XV contains the maximal value of $|\psi|$ on the inner collocation points $M_1 \cdot M_1^B$ represents the results in [4]. Table XVI shows the corresponding results for $|\omega|$ on the collocation points M_2 on the side $\bar{y} = 1$.

Note that M_2 does not give a precise account of the maximum of $|\omega|$ because of the strong variation of the vorticity on the edge $\bar{y} = 1$ and the uneven spacing of the collocation points. But since the approximation on $\bar{y} = 1$ is done by a polynomial defined at every $\bar{x} \in [0, 1]$ we have divided the space into 201 equally spaced points on this edge. The corresponding values of $|\omega|$ are presented in Table XVII (denoted M_3).

TABLE XIV
Critical Time Step $\triangle t_c$ (with an error of $\pm 10^{-3}$)

N	$\mathrm{Re} = 100$	$\mathrm{Re} = 400$
16	0.303	0.104
20	0.250	0.074
24	0.234	0.056

TABLE XV
Maximal Value of $|\psi|^a$

	Re = 100		Re = 400	
N	M_1^B	M_1	M_1^B	M_1
16	8.3160×10^{-2} $(0.40 - 0.78)$	8.3160×10^{-2} $(0.40 - 0.78)$	8.5777×10^{-2} $(0.40 - 0.60)$	8.5452×10^{-2} $(0.40 - 0.60)$
20	8.2694×10^{-2} $(0.42 - 0.73)$	8.2695×10^{-2} $(0.42 - 0.73)$	8.5192×10^{-2} $(0.42 - 0.58)$	8.5213×10^{-2} $(0.42 - 0.58)$
24	8.3315×10^{-2} $(0.37 - 0.75)$	8.3315×10^{-2} $(0.37 - 0.75)$	8.5716×10^{-2} $(0.43 - 0.63)$	8.5715×10^{-2} $(0.43 - 0.63)$
32	8.3402×10^{-2} $(0.40 - 0.74)$	8.3402×10^{-2} $(0.40 - 0.74)$	8.5480×10^{-2} $(0.40 - 0.60)$	8.4007×10^{-2} $(0.40 - 0.65)$

[a] The coordinates are given in parentheses.

TABLE XVI
Maximal Value of $|\omega|^a$

	Re = 100		Re = 400	
N	M_2^B	M_2	M_2^B	M_2
16	13.3467 (0.60)	13.3442 (0.60)	24.7759 (0.60)	24.6541 (0.60)
20	13.1759 (0.65)	13.1762 (0.65)	24.6268 (0.65)	24.6243 (0.65)
24	13.4226 (0.63)	13.4228 (0.63)	24.9157 (0.63)	24.9143 (0.63)
32	13.3423 (0.60)	13.3422 (0.60)	24.7845 (0.65)	24.9783 (0.65)

[a] The coordinates are given in parentheses.

TABLE XVII
Maximal Value of $|\omega|^a$

	Re = 100		Re = 400	
N	M_3^B	M_3	M_3^B	M_3
16	13.4476 (0.620)	13.4434 (0.620)	25.1604 (0.625)	25.0222 (0.625)
20	13.4441 (0.620)	13.4441 (0.620)	24.9273 (0.630)	24.9241 (0.630)
24	13.4446 (0.610)	13.4565 (0.620)	24.9148 (0.630)	24.9010 (0.625)
32	13.4448 (0.620)	13.4430 (0.620)	24.9109 (0.630)	25.1123 (0.625)

[a] The coordinates are given in parentheses.

8. CONCLUSIONS

We have presented and discussed the splitting for the unsteady Stokes equations whereas we decoupled the system into Helmholtz equations for the velocity and an equation with the pseudo-Laplacian for the pressure. The spatial discretization is performed by a $\mathbb{P}_N \times \mathbb{P}_{N-1}$ Chebyshev collocation-type method by using staggered grids. Then we have extended our splitting scheme to the Navier–Stokes equations. Our discretization is free of spurious modes and we have found a good preconditioner for the ill-conditioned pseudo-Laplacian. While we have lost some accuracy in the pressure, good results for the approximation of the velocity are achieved.

REFERENCES

1. K. Arrow, L. Hurwicz, and H. Uzawa, *Studies in Nonlinear Programming* (Stanford University Press, Stanford, CA, 1968).
2. I. Babuška and M. Suri, The p- and hp-versions of the finite element method: An overview, *Comput. Meth. Appl. Mech. Eng.* **80**, 5 (1990).
3. C. Bernardi and Y. Maday, A collection method over staggered grids for the Stokes problem, *Int. J. Numer. Meth. Fluids* **8**, 537 (1988).
4. O. Botella, On the solution of the Navier–Stokes equations using Chebyshev projection schemes with third-order accuracy in time, *Comput. Fluids* **26**, 107 (1997).
5. F. Brezzi and M. Fortin, *Mixed and Hybrid Finite Element Methods* (Springer-Verlag, New York, 1991).
6. M. O. Bristeau, R. Glowinski, and J. Periaux, Numerical methods for the Navier–Stokes equations. Applications to the simulation of compressible and incompressible viscous flows, *Comput. Phys. Rep.* **6**, 73 (1987).
7. C. Canuto, M. Y. Hussaini, A. Quarteroni, and T. A. Zhang, *Spectral Methods in Fluid Dynamics*, Springer Series Comput. Phys. (Springer-Verlag, Berlin, Heidelberg, New York, 1989).
8. P. Deuflhard and F. Bornemann, *Numerische Mathematik II* (De Gruyter, Berlin, 1994).
9. G. Engeln-Müllges and F. Uhlig, *Numerical Algorithms with C* (Springer-Verlag, Berlin, 1996).
10. V. Girault and P. A. Raviart, *Finite Element Approximation of the Navier–Stokes-Equations* (Springer-Verlag, New York, 1988).
11. D. Gottlieb and A. Lustman, The spectrum of the Chebyshev collocation operator for the heat equation, *SIAM J. Numer. Anal.* **20**, 909 (1983).
12. W. Heinrichs, Splitting techniques for the pseudospectral approximation of the unsteady Stokes equations, *SIAM J. Numer. Anal.* **30**, 19 (1993).
13. W. Heinrichs, Splitting techniques for the unsteady Stokes equations, *SIAM J. Numer. Anal.* **35**(4), 1646 (1998).
14. R. A. Horn and C. R. Johnson, *Topics in Matrix Analysis* (Cambridge University Press, Cambridge, UK, 1991).
15. Y. Maday, D. Merion, A. T. Patera, and E. Rønquist, Analysis of iteration methods for the steady and unsteady Stokes problems: Applications to spectral elements discretizations, *SIAM J. Sci. Comput.* **14**, 310 (1993).
16. Y. Maday, A. T. Patera, and E. Rønquist, An operator-integration-factor splitting method for time-dependent problem: Application to incomplressible fluid flow, *J. Sci. Comput.* **5**, 263 (1990).
17. A. Quarteroni and A. Valli, *Numerical Approximation of Partial Differential Equations* (Springer-Verlag, Berlin, 1994).
18. E. Rønquist, *Optimal Spectral Element Methods for the Unsteady Three-dimensional Incompressible Navier–Stokes Equations* Ph.D. thesis (Massachusetts Institute of Technology, Cambridge, MA, 1988).
19. R. Temam, *Navier–Stokes-Equations. Theory and Numerical Analysis* (North-Holland, Amsterdam, 1984).